

Eocene global warming events driven by ventilation of oceanic dissolved organic carbon

Philip F. Sexton^{1,2,†}, Richard D. Norris¹, Paul A. Wilson², Heiko Pälike², Thomas Westerhold³, Ursula Röhl³, Clara T. Bolton^{2,†} & Samantha Gibbs²

'Hyperthermals' are intervals of rapid, pronounced global warming known from six episodes within the Palaeocene and Eocene epochs (~65–34 million years (Myr) ago)^{1–13}. The most extreme hyperthermal was the ~170 thousand year (kyr) interval² of 5–7 °C global warming³ during the Palaeocene–Eocene Thermal Maximum (PETM, 56 Myr ago). The PETM is widely attributed to massive release of greenhouse gases from buried sedimentary carbon reservoirs^{1,3,6,11,14–17}, and other, comparatively modest, hyperthermals have also been linked to the release of sedimentary carbon^{3,6,11,16,17}. Here we show, using new 2.4-Myr-long Eocene deep ocean records, that the comparatively modest hyperthermals are much more numerous than previously documented, paced by the eccentricity of Earth's orbit and have shorter durations (~40 kyr) and more rapid recovery phases than the PETM. These findings point to the operation of fundamentally different forcing and feedback mechanisms than for the PETM, involving redistribution of carbon among Earth's readily exchangeable surface reservoirs rather than carbon exhumation from, and subsequent burial back into, the sedimentary reservoir. Specifically, we interpret our records to indicate repeated, large-scale releases of dissolved organic carbon (at least 1,600 gigatonnes) from the ocean by ventilation (strengthened oxidation) of the ocean interior. The rapid recovery of the carbon cycle following each Eocene hyperthermal strongly suggests that carbon was re-requested by the ocean, rather than the much slower process of silicate rock weathering proposed for the PETM^{1,3}. Our findings suggest that these pronounced climate warming events were driven not by repeated releases of carbon from buried sedimentary sources^{3,6,11,16,17}, but, rather, by patterns of surficial carbon redistribution familiar from younger intervals of Earth history.

Earth's climate attained its warmest state of the past 80 Myr during the early Palaeogene period (~45–65 Myr ago) (Fig. 1a). Centred within this interval at 56 Myr ago, the PETM marks a rapid excursion of 2.5‰ to >3.0‰ in the carbon isotope composition ($\delta^{13}\text{C}$) of marine carbonates^{1,3} and terrestrial organic matter concurrent with widespread dissolution of carbonate sediments^{1,3} and deep ocean warming by 6–7 °C (ref. 3). The source of carbon triggering this large perturbation to the exchangeable carbon reservoirs at Earth's surface (ocean, atmosphere and biosphere) is widely acknowledged to have come from an 'external' sedimentary reservoir(s)^{1,3,6,11,14–17}. A long-standing hypothesis attributes this event to the release of massive amounts of methane from sedimentary gas hydrate deposits^{1,6,11,14–16}, with attendant oxidation to CO_2 causing climate warming through a greenhouse feedback³. Because of the relative rapidity of its onset, and the estimated quantity of sedimentary-sourced carbon involved, the PETM has attracted interest as a natural analogue to the current anthropogenic perturbation to Earth's surficial carbon cycle.

In recent years, six transient warming events comparable in character to the PETM, but less extreme in magnitude and duration, have been discovered throughout the early Palaeogene (at about 65.2, 58.2, 53.7,

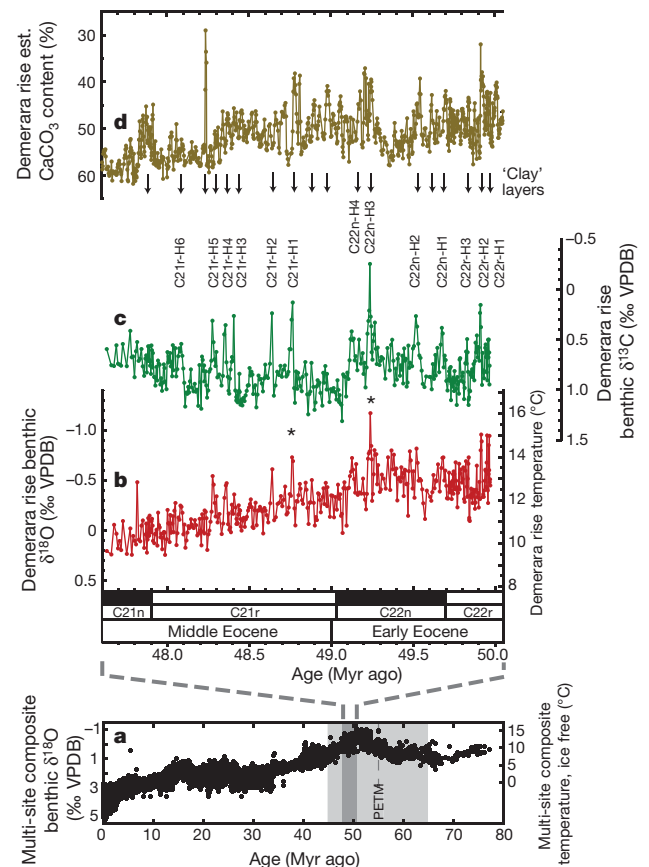


Figure 1 | High-resolution records across the early Eocene to middle Eocene transition from ODP Site 1258, Demerara rise, tropical Atlantic. **a**, Deep sea benthic foraminifer composite $\delta^{18}\text{O}$ data for the past 80 Myr from multiple sites^{3,8,10} (full list of data sources in Supplementary Note 1). PETM, Palaeocene–Eocene Thermal Maximum. Light grey shaded area, early Palaeogene period (45–65 Myr ago). Dark grey shaded box, study interval for this work. $\delta^{18}\text{O}$ -temperature scale is for ice-free conditions⁵ (–1.27‰ VPDB). **b–d**, Data from ODP Site 1258, Demerara rise, with an astronomically calibrated age model (Methods). **b**, Benthic foraminifer $\delta^{18}\text{O}$ and calculated palaeotemperatures (Methods). All benthic $\delta^{18}\text{O}$ data in **a** and **b** are corrected to equilibrium calcite. **c**, Benthic foraminifer $\delta^{13}\text{C}$. Note the repeated, rapid excursions to lower values. Events numbered (according to the magnetochron within which they occur) are those with a $\delta^{13}\text{C}$ excursion exceeding 0.7‰. Black arrows mark the stratigraphic positions of clay-rich CaCO_3 dissolution horizons ($n = 18$) made visible by their brown colour in the Demerara rise sedimentary sequence, 13 of which correspond precisely to the numbered, rapid excursions to lower benthic $\delta^{13}\text{C}$ values in **c**. The remaining 5 clay layers are also associated with trends to lower $\delta^{13}\text{C}$, but of noticeably smaller magnitude. **d**, Estimated CaCO_3 content of sediment. Asterisks denote individual 'hyperthermal' events shown in more detail in Fig. 2.

¹Scripps Institution of Oceanography, University of California, San Diego, La Jolla, California 92093, USA. ²National Oceanography Centre Southampton, University of Southampton, European Way, Southampton SO14 3ZH, UK. ³MARUM — Center for Marine Environmental Sciences, University of Bremen, Leobener Strasse, 28359 Bremen, Germany. [†]Present addresses: Department of Earth and Environmental Sciences, The Open University, Milton Keynes MK7 6AA, UK (P.F.S.); Departamento de Geología, Universidad de Oviedo, 33005 Oviedo, Spain (C.T.B.).

53.2, 52.5 and 41.8 Myr ago^{4–13}). These ‘hyperthermals’⁴ have not been found during the later and cooler part of the Eocene (after ~40 Myr ago) (Fig. 1a). The number of these hyperthermals, and the relative temporal spacing between some of them, is suggestive of the operation of common mechanisms^{5,6,11}. Although various mechanisms have been proposed for the origin of these comparatively modest events^{5,7,12}, it is widely considered that they too were triggered by large-scale releases of carbon from sedimentary reservoirs^{3,6,11,16,17}, probably methane hydrates^{3,6,11,16}. Yet, the typical magnitude of the $\delta^{13}\text{C}$ anomalies across known hyperthermals (up to ~1.0‰) is not unusual for $\delta^{13}\text{C}$ records from the better chronicled Neogene period and, more importantly, these anomalies are not so large that they necessitate a source of carbon that is as extremely isotopically depleted as methane hydrate ($\delta^{13}\text{C} = -60\text{‰}$).

A new 2.4-Myr-long benthic foraminifer stable isotope record (Supplementary Discussion) from Demerara rise in the tropical western Atlantic Ocean (Ocean Drilling Program Site 1258) shows that events exhibiting the characteristics of previously identified hyperthermals are abundant in the Palaeogene deep-sea palaeoceanographic record. Spanning the early Eocene to middle Eocene transition (47.6–50.0 Myr ago), these records indicate that average temperatures in the early Eocene equatorial Atlantic were 12–14 °C at about 3,000 m (ref. 8) palaeo-water depth (Fig. 1b). This warm deep ocean state is punctuated by 13 excursions to lower $\delta^{18}\text{O}$ values indicative of short-term warming by ~2–4 °C (Figs 1b, 2; events numbered in Fig. 1c), each lasting about 40 kyr and spaced about 100–400 kyr apart (Supplementary Discussion). These transient warming events develop very rapidly (<5–10 kyr) and decay to ‘background’ temperatures more slowly (over ~30 kyr) (Fig. 2).

Our accompanying benthic foraminifer $\delta^{13}\text{C}$ record shows that each warming event is marked by an excursion to lower $\delta^{13}\text{C}$ values by 0.7–1.0‰ (Fig. 1c). Where planktic records are available for the most prominent negative excursions in the benthic $\delta^{13}\text{C}$ record, these also reveal negative $\delta^{13}\text{C}$ excursions of 0.6–0.9‰ (Fig. 2), suggesting that these events represent whole-ocean decreases in $\delta^{13}\text{C}$ of total dissolved inorganic carbon.

All of the benthic $\delta^{13}\text{C}$ excursions are associated with brown clay-rich layers at Demerara rise (arrows in Fig. 1), a hallmark of other reported early Palaeogene hyperthermals^{1,6,7,10,12,13}, that suggests increased calcium carbonate (CaCO_3) dissolution. Clay layers occur in other parts of the record as well, associated with $\delta^{13}\text{C}$ excursions of smaller magnitude than our numbered excursions (Fig. 1c). This suggests that the largest hyperthermals (those numbered in Fig. 1c) represent prominent end-members in a spectrum of carbon cycle perturbations that scale up from orbitally paced ‘background’ cycles. Records of estimated CaCO_3 concentrations from Demerara rise (palaeo-water depth ~3 km; ref. 8)

and sites in the southern Atlantic and central Pacific oceans (palaeo-water depths ~3 and 2 km, respectively; Supplementary Discussion) reveal synchronous, globally widespread decreases in CaCO_3 accumulation (Supplementary Fig. 2e–g). Calculations of CaCO_3 dissolution associated with the clay layers in the Atlantic and Pacific (Supplementary Discussion) indicate that CaCO_3 dissolution events (Fig. 3b–d) are coeval with the large negative benthic $\delta^{13}\text{C}$ excursions at Demerara rise (Fig. 3a). This correspondence strongly suggests that global increases in deep ocean acidity were associated with intervals of isotopically ‘light’ carbon pervading the world’s oceans.

These perturbations to oceanic carbon cycling could have been fuelled by carbon input from a number of different sources. Besides methane hydrates, erosion of sedimentary organic carbon (C_{org}) could supply carbon with a $\delta^{13}\text{C}$ composition (about -25‰) that is less depleted than that of methane (-60‰). A third potential source is redistribution of carbon within the exchangeable reservoirs at Earth’s surface (ocean, atmosphere and biosphere). Redistribution of isotopically light carbon among the internal, readily exchangeable reservoirs should produce $\delta^{13}\text{C}$ excursions with fundamentally different size, shape, duration and recovery trends than carbon input from an external, sedimentary reservoir.

Mass balance considerations (assuming masses of Eocene carbon reservoirs similar to modern) dictate that the ~1‰ $\delta^{13}\text{C}$ excursions we observe are compatible with injection of a mass of carbon from methane hydrates (-60‰) of about 650 gigatonnes (Gt). But this mass of carbon is far too small to have driven our corresponding deep ocean warmings of 2–4 °C (Figs 1b, 2), particularly given that deep ocean warming of 6–7 °C at the PETM³ was triggered by release of ~3,000 to 6,000 Gt of carbon¹⁷. The large and widespread increases in CaCO_3 dissolution associated with our hyperthermals also appear to demand a much larger input of carbon than the 650 Gt permitted by a methane hydrate source.

The $\delta^{13}\text{C}$ composition of sedimentary C_{org} (about -25‰) permits a much larger carbon release (~1,600 Gt) to be accommodated within the observed 1‰ $\delta^{13}\text{C}$ excursions of hyperthermals, but problems also exist with this explanation. The ~140-kyr residence time of carbon in Earth’s exchangeable reservoirs^{14,15} suggests that the liberation of a substantial quantity of isotopically light carbon from an external, deeply buried source should have a long imprint on oceanic and atmospheric $\delta^{13}\text{C}$ (approaching the residence time)¹⁸ until the excess carbon is ultimately sequestered back into the long-term sedimentary carbon reservoir by weathering reactions¹⁸. This behaviour is demonstrated at the PETM, which shows a $\delta^{13}\text{C}$ excursion ~170 kyr in duration² with a very long recovery ‘tail’^{1,3,5,11} that produces a very asymmetrical excursion and reflects the long timescales required for weathering to draw down this external CO_2 and return it to the sedimentary reservoir as CaCO_3 .

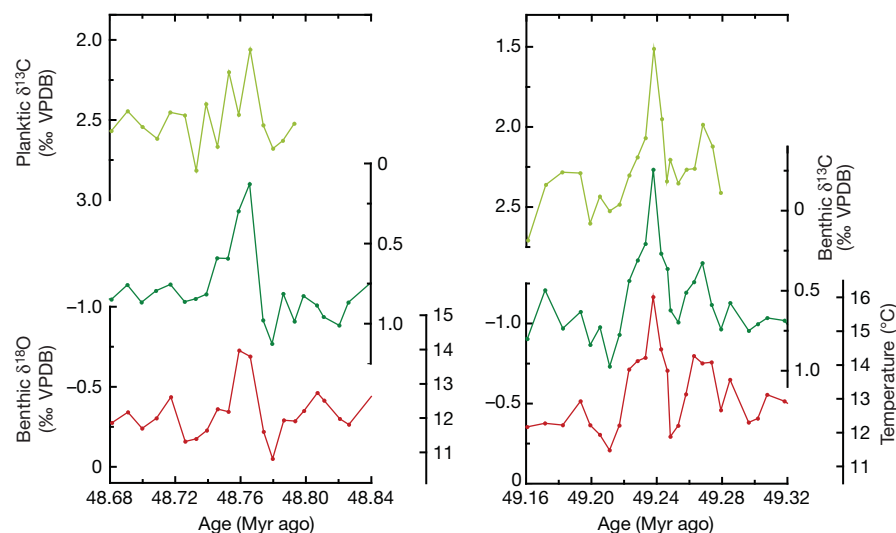


Figure 2 | Details of stable isotope data from ODP Site 1258 across two ‘hyperthermal’ events. Isotope data are from Fig. 1; the two events are marked by asterisks in Fig. 1. Labels on the x-axes are at 40-kyr spacing, highlighting the similarity of the duration (that is, ‘trough to trough’) of these events to the obliquity frequency. We define the ‘onset’ phase of events as ‘trough to peak’, with their ‘recovery’ being ‘peak to trough’. Red, benthic foraminifer $\delta^{18}\text{O}$. Dark green, benthic $\delta^{13}\text{C}$. Light green, planktic $\delta^{13}\text{C}$.

However, our $\delta^{13}\text{C}$ excursions are too short (only ~ 40 -kyr total duration), and return to pre-excursion values too fast (within 30 kyr; Figs 1c, 2) and to a post-excursion baseline that is isotopically no different from pre-excursion, to be compatible with large-scale liberation of isotopically light carbon from a buried reservoir. The recoveries seen for other hyperthermals^{5,6,8,10–13} are also too rapid to represent sequestration of substantial amounts of sedimentary-sourced carbon.

The incompatibility of hyperthermals with external, sedimentary carbon sources indicates that the carbon that fuelled them was probably redistributed within the readily exchangeable reservoirs at Earth's surface. Although some of this carbon may have come from the terrestrial biosphere, possibly acting as a feedback to a primary source, we are unable to test this possibility with our data at present. However, the oceans are by far the largest of these exchangeable reservoirs; the present-day oceans contain 13 times as much carbon as the combined biosphere and atmosphere—all told about 40,000 Gt of carbon. Today, this mass of oceanic carbon comprises about 37,500 Gt of dissolved inorganic carbon ($\delta^{13}\text{C} \approx 0\text{‰}$), 30 Gt of particulate organic carbon ($\delta^{13}\text{C} \approx -25\text{‰}$) and 700–1,800 Gt of dissolved organic carbon (DOC; $\delta^{13}\text{C} \approx -25\text{‰}$). Redistribution of a mass of isotopically light carbon equivalent to the entire modern DOC reservoir ($\sim 1,600$ Gt C) would be required to produce the $\sim 1.0\text{‰}$ $\delta^{13}\text{C}$ excursions seen for our events and previously reported ones^{5,6,8,10–13}, but the DOC reservoir size would probably grow, perhaps many fold, under more oxygen-depleted deep ocean conditions. Within the oceans, the two principal reservoirs for storing large quantities of carbon are marginal basins or the abyssal ocean. Because of its sheer size, the deep abyssal reservoir of carbon has long been implicated in the regular fluctuations (~ 100 parts per million by volume, p.p.m.v.) of atmospheric CO_2 and $\sim 5^\circ\text{C}$ surface temperature changes seen across the late Pleistocene glacial cycles. It has recently become clear that the abyssal Southern Ocean has played a pivotal role in Pleistocene carbon cycling through its gradual amassing of respired CO_2 during glacials^{19–21} and subsequent release via increased ventilation^{19–21} during deglaciation.

Several observations suggest that the source of CO_2 fuelling Eocene hyperthermals was the abyssal ocean. First, our dissolution records provide clues to the location of CO_2 storage in the exchangeable carbon reservoirs. Numerical modelling experiments indicate that CaCO_3 dissolution should be most intense close to the source of carbon release¹⁵. In our estimates of CaCO_3 dissolution, dissolution intensity appears to be consistently highest in the southern Atlantic (Fig. 3e) compared to other sites. This finding raises the possibility that the abyssal reservoir of carbon was located in the Southern Ocean. Second, all of our hyperthermals have a duration of about 40 kyr (Fig. 1b, c, Fig. 2). The similarity of this period to the 41-kyr obliquity cycle suggests that the forcing for individual hyperthermal events had its origin at high latitudes. This observation is consistent with an obliquity pacing of high latitude surface ocean stratification controlling carbon ventilation (via oxygenation), as proposed for the last deglaciation²².

If the source of CO_2 driving Eocene hyperthermals was the deep ocean, a number of observations suggest that our Eocene sites may be somewhat analogous to intermediate-depth sites during Pleistocene glacials that were located above a deeper CO_2 storage reservoir^{19,23}. First, the absence before our hyperthermals of either gradually decreasing benthic $\delta^{13}\text{C}$ or increasing dissolution intensity (Figs 1c, 2) indicates that our mid-depth (2–3 km) sites did not 'sense' the gradual ($\sim 10^4$ – 10^5 year) build-up of a CO_2 reservoir until its final release. Second, early Eocene sediments from lower abyssal depths reveal lithological indications for relatively long intervals of carbon storage followed by short, intermittent intervals of carbon release (Supplementary Discussion).

The relatively long ~ 100 -kyr or 400-kyr intervals between CO_2 release events (Fig. 1) would suggest an apparent means by which a large Eocene abyssal reservoir of DOC could intermittently grow. Yet increases in the DOC reservoir are difficult to achieve solely by long residence times of deep water, owing to progressive bacterial

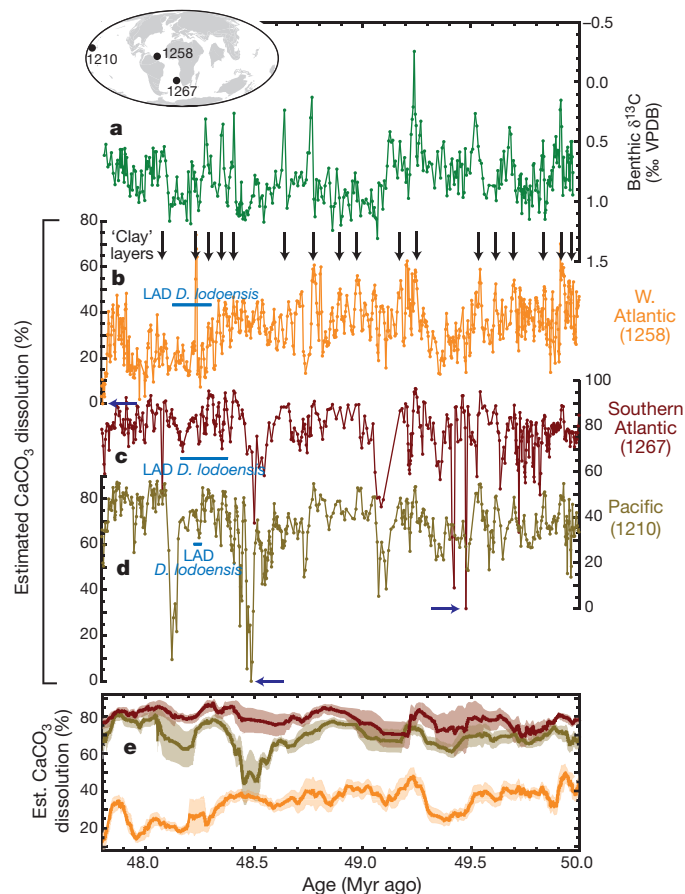


Figure 3 | Eocene records of benthic foraminifer $\delta^{13}\text{C}$ and CaCO_3 dissolution. **a**, Benthic $\delta^{13}\text{C}$ from Fig. 1c (Demerara rise, ODP Site 1258, tropical Atlantic). **b–d**, Records of calculated CaCO_3 dissolution from ODP Site 1258 (**b**), ODP Site 1267, southern Atlantic (**c**), ODP Site 1210, Pacific (**d**), and smoothed versions (25-point running mean) of all three (**e**). Shaded envelopes in **e** are 1σ variance about the mean. Simultaneous increases in CaCO_3 dissolution occur at all three sites and are marked by visible, brown 'clay' layers in sediment cores at each of the sites (marked by solid black arrows). Blue arrows mark our assumed 'zero-dissolution points' for each site (that is, the primary, unaltered fractional component of CaCO_3 in the sediment; Supplementary Fig. 2 and Supplementary Discussion). Light blue horizontal bars mark the interval at each site within which the last appearance datum (LAD) of the nannofossil *Discoaster lodoensis* occurs, providing a primary point of stratigraphic correlation between sites. Inset map from ODSN Plate Tectonic Reconstruction Service.

respiration primarily of young, labile DOC components during the water mass ageing process²⁴. However, under anoxic conditions, DOC may build up. For example, concentrations of DOC in the anoxic depths ($>2,000$ m) of the modern Black Sea are ~ 2.5 times those of the global deep ocean²⁵. An early Eocene decoupling of marine burial rates of C_{org} versus pyrite indicates that the ocean during this interval regularly experienced pronounced anoxia²⁶. We suggest that this persistent anoxia, perhaps in the severely undersampled early Eocene abyss, and at least partly driven by the lower solubility of oxygen at warmer abyssal temperatures (Fig. 1a, b), would have promoted the build-up of a reservoir of DOC large enough to have fuelled hyperthermal carbon releases of $\sim 1,600$ Gt. Anoxia in the Eocene abyss is consistent with modelling projections for the next few millennia indicating a large reduction in abyssal ventilation (by up to 75%)²⁷ in response to climate warming induced by an 'anthropogenic' atmospheric partial pressure of CO_2 (1,700 p.p.m.v.) similar to that of the early Eocene.

Further support for the existence of a larger-than-modern Eocene deep (>3 km) ocean reservoir of DOC is found in surface-to-deep profiles of seawater temperature and $\delta^{13}\text{C}$ reconstructed from multiple species of planktic and benthic foraminifera (Supplementary Fig. 4). In

comparison to recent core-top data, Eocene data reveal a greater total surface-to-seafloor $\delta^{13}\text{C}$ difference along with a steeper vertical gradient of $\delta^{13}\text{C}$ of dissolved inorganic carbon versus temperature (Supplementary Fig. 4). These two observations are respectively consistent with a deeper mean C_{org} remineralization depth and an intensification of organic carbon production in the upper ocean. The resultant greater Eocene vertical export flux of carbon may have allowed the unremineralized DOC component to build up to higher-than-modern levels. Furthermore, the much greater species diversity of calcareous nannofossils relative to diatoms throughout the early Palaeogene²⁸ may have accelerated the abyssal transfer of C_{org} from the surface owing to the greater ballasting efficiency of CaCO_3 relative to opal²⁹. A major switch to greater species diversity of diatoms relative to calcareous nannofossils (at ~ 40 Myr ago)²⁸ coincides with the last documented early Cenozoic 'hyperthermal' event¹⁰.

Although the PETM must have been fuelled by carbon injection from an external, sedimentary source(s), we suggest that astronomically paced changes in ocean ventilation (oxygenation) of DOC may explain the numerous less extreme hyperthermals that are being discovered^{14–13} throughout the early Palaeogene. CO_2 ventilation is a viable mechanism with which to sustain the repeated, frequent carbon releases that define hyperthermals over a geologically extended interval (Fig. 1b, c)^{4–13} because the recharge times of the abyssal ocean (via decomposition of organic matter) are rapid compared to the slow, multi-million-year filling of sedimentary methane hydrate reservoirs³⁰. The extraordinarily warm mean state of the Palaeogene oceans (Fig. 1a, b) also raises the question as to whether large-scale methane hydrate reservoirs would even have existed at this time³⁰. Despite the extreme nature of these repeated Palaeogene climate warming events, our findings indicate that they were driven by changes in storage of carbon within the oceans, in a manner somewhat familiar from younger intervals of Earth history.

METHODS SUMMARY

$\delta^{18}\text{O}$ and $\delta^{13}\text{C}$ data were generated using mono-specific analyses of the benthic foraminifers *Cibicidoides subspiratus* and *Cibicidoides eocenus* at the National Oceanography Centre, University of Southampton, Southampton. High resolution Eocene records of CaCO_3 concentrations were calculated, by regression, using sediment physical property data and measurements of sediment CaCO_3 content. We developed an astronomically calibrated age model for Site 1258 (Demerara rise). Detailed chronologies for sites 1267 and 1210 were generated by tuning clear, correlatable events in their respective CaCO_3 (%) records to the astronomically calibrated CaCO_3 (%) record from Site 1258.

Full Methods and any associated references are available in the online version of the paper at www.nature.com/nature.

Received 6 August 2010; accepted 12 January 2011.

- Zachos, J. C. *et al.* Rapid acidification of the ocean during the Paleocene-Eocene thermal maximum. *Science* **308**, 1611–1615 (2005).
- Röhl, U., Westerhold, T., Bralower, T. J. & Zachos, J. C. On the duration of the Paleocene-Eocene thermal maximum (PETM). *Geochem. Geophys. Geosyst.* **8**, Q12002 (2007).
- Zachos, J. C., Dickens, G. R. & Zeebe, R. E. An early Cenozoic perspective on greenhouse warming and carbon-cycle dynamics. *Nature* **451**, 279–283 (2008).
- Thomas, E., Zachos, J. C. & Bralower, T. J. in *Warm Climates in Earth History* (eds Huber, B., MacLeod, K. & Wing, S.) 132–160 (Cambridge Univ. Press, 2000).
- Cramer, B. S., Wright, J. D., Kent, D. V. & Aubry, M. P. Orbital climate forcing of $\delta^{13}\text{C}$ excursions in the late Paleocene-early Eocene (chons C24n-C25n). *Paleoceanography* **18**, 1097, doi:10.1029/2003PA000909 (2003).
- Lourens, L. J. *et al.* Astronomical pacing of late Palaeocene to early Eocene global warming events. *Nature* **435**, 1083–1087 (2005).
- Petrizzo, M. R. An early late Paleocene event on Shatsky Rise, northwest Pacific Ocean (ODP Leg 198): evidence from planktonic foraminiferal assemblages. *Proc. ODP Sci. Res.* **198**, 1–29 (2005).
- Sexton, P. F., Wilson, P. A. & Norris, R. D. Testing the Cenozoic multisite composite $\delta^{18}\text{O}$ and $\delta^{13}\text{C}$ curves: new monospecific Eocene records from a single locality, Demerara Rise (Ocean Drilling Program Leg 207). *Paleoceanography* **21**, PA2019, doi:10.1029/2005PA001253 (2006).
- Westerhold, T. *et al.* On the duration of magnetochrons C24r and C25n and the timing of early Eocene global warming events: implications from the Ocean Drilling Program Leg 208 Walvis Ridge depth transect. *Paleoceanography* **22**, PA2201, doi:10.1029/2006PA001322 (2007).

- Edgar, K. M., Wilson, P. A., Sexton, P. F. & Sugauma, Y. No extreme bipolar glaciation during the main Eocene calcite compensation shift. *Nature* **448**, 908–911 (2007).
- Nicolo, M. J., Dickens, G. R., Hollis, C. J. & Zachos, J. C. Multiple early Eocene hyperthermals: their sedimentary expression on the New Zealand continental margin and in the deep sea. *Geology* **35**, 699–702 (2007).
- Quillévéré, F., Norris, R. D., Kroon, D. & Wilson, P. A. Transient ocean warming and shifts in carbon reservoirs during the early Danian. *Earth Planet. Sci. Lett.* **265**, 600–615 (2008).
- Stap, L. *et al.* High-resolution deep-sea carbon and oxygen isotope records of Eocene Thermal Maximum 2 and H2. *Geology* **38**, 607–610 (2010).
- Dickens, G. R., O'Neil, J. R., Rea, D. K. & Owen, R. M. Dissociation of oceanic methane hydrate as a cause of the carbon isotope excursion at the end of the Paleocene. *Paleoceanography* **10**, 965–971 (1995).
- Dickens, G. R. Methane oxidation during the late Palaeocene thermal maximum. *Bull. Soc. Geol. Fr.* **171**, 37–49 (2000).
- Dickens, G. R. Rethinking the global carbon cycle with a large, dynamic and microbially mediated gas hydrate capacitor. *Earth Planet. Sci. Lett.* **213**, 169–183 (2003).
- Panchuk, K., Ridgwell, A. & Kump, L. R. Sedimentary response to Paleocene-Eocene Thermal Maximum carbon release: a model-data comparison. *Geology* **36**, 315–318 (2008).
- Archer, D. Fate of fossil fuel CO_2 in geologic time. *J. Geophys. Res.* **110**, C09S05, doi:10.1029/2004JC002625 (2005).
- Hodell, D. A., Venz, K. A., Charles, C. D. & Ninnemann, U. S. Pleistocene vertical carbon isotope and carbonate gradients in the South Atlantic sector of the Southern Ocean. *Geochem. Geophys. Geosyst.* **4** (1), 1004, doi:10.1029/2002GC000367 (2003).
- Toggweiler, J. R., Russell, J. L. & Carson, S. R. Midlatitude westerlies, atmospheric CO_2 , and climate change during the ice ages. *Paleoceanography* **21**, PA2005, doi:10.1029/2005PA001154 (2006).
- Skinner, L. C., Fallon, S., Waelbroeck, C., Michel, E. & Barker, S. Ventilation of the deep Southern Ocean and deglacial CO_2 rise. *Science* **328**, 1147–1151 (2010).
- Sigman, D. M., de Boer, A. M. & Haug, G. H. in *Past and Future Changes of the Oceanic Meridional Overturning Circulation: Mechanisms and Impacts* (eds Schmittner, A., J., Chiang, H. C. & Hemming, S. R.) 335–350 (AGU Geophysical Monograph 173, American Geophysical Union, 2007).
- Marchitto, T. M., Lehman, S. J., Ortiz, J. D., Fluckiger, J. & van Geen, A. Marine radiocarbon evidence for the mechanism of deglacial atmospheric CO_2 rise. *Science* **316**, 1456–1459 (2007).
- Hansell, D. A. & Carlson, C. A. Deep-ocean gradients in the concentration of dissolved organic carbon. *Nature* **395**, 263–266 (1998).
- Ducklow, H. W., Hansell, D. A. & Morgan, J. A. Dissolved organic carbon and nitrogen in the western Black Sea. *Mar. Chem.* **105**, 140–150 (2007).
- Kurtz, A. C., Kump, L. R., Arthur, M. A., Zachos, J. C. & Paytan, A. Early Cenozoic decoupling of the global carbon and sulfur cycles. *Paleoceanography* **18**, 1090, doi:10.1029/2003PA000908 (2003).
- Schmittner, A., Oeschies, A., Matthews, H. D. & Galbraith, E. D. Future changes in climate, ocean circulation, ecosystems, and biogeochemical cycling simulated for a business-as-usual CO_2 emission scenario until year 4000 AD. *Glob. Biogeochem. Cycles* **22**, GB1013, doi:10.1029/2007GB002953 (2008).
- Falkowski, P. G. *et al.* The evolution of modern eukaryotic phytoplankton. *Science* **305**, 354–360 (2004).
- Klaas, C. & Archer, D. E. Association of sinking organic matter with various types of mineral ballast in the deep sea: implications for the rain ratio. *Glob. Biogeochem. Cycles* **16** (4), 1116, doi:10.1029/2001GB001765 (2002).
- Buffett, B. & Archer, D. Global inventory of methane clathrate: sensitivity to changes in the deep ocean. *Earth Planet. Sci. Lett.* **227**, 185–199 (2004).

Supplementary Information is linked to the online version of the paper at www.nature.com/nature.

Acknowledgements We thank M. Bolshaw for laboratory assistance and the shipboard party and crew of Ocean Drilling Program (ODP) Leg 207 for a successful drilling expedition. We thank H. Brinkhuis, G. Dickens, G. Foster, M. Huber, S. Kirtland, D. Kroon, L. Kump, E. Rohling and J. Zachos for discussions. This research used samples and data provided by the ODP. ODP (now IODP) is sponsored by the US NSF and participating countries under the management of JOI, Inc. We thank W. Hale and A. Wülbels (IODP) for assistance with sediment core sampling. Financial support for this research was provided by a European Commission Marie Curie Outgoing International Fellowship (P.F.S.), a Leverhulme Trust Fellowship (P.F.S.), a Natural Environment Research Council UK ODP grant (P.A.W. and P.F.S.), a Philip Leverhulme Prize (H.P.), the DFG-Leibniz Center for Surface Process and Climate Studies at the University of Potsdam, and the DFG (U.R. and T.W.).

Author Contributions P.F.S. and P.A.W. designed and instigated the research. P.F.S. and C.T.B. picked foraminifera. P.F.S. and P.A.W. generated stable isotope records. P.F.S. and H.P. generated the estimated CaCO_3 content records and constructed age models. P.F.S. conducted stratigraphic correlations between the various drill sites. T.W. and U.R. modified the spliced sedimentary section at Demerara rise. S.G. generated biostratigraphic data for Demerara rise. P.F.S. and R.D.N. wrote the manuscript. P.A.W., H.P., T.W. and U.R. commented on the manuscript.

Author Information Reprints and permissions information is available at www.nature.com/reprints. The authors declare no competing financial interests. Readers are welcome to comment on the online version of this article at www.nature.com/nature. Correspondence and requests for materials should be addressed to P.F.S. (P.F.Sexton@open.ac.uk).

METHODS

Stable isotope data. Benthic foraminifera were picked from the 250–400 μm size fraction. Stable isotope data were generated at the National Oceanography Centre, University of Southampton, Southampton, using a Europa Geo 20-20 mass spectrometer equipped with an automatic carbonate preparation system. For each analysis, between 4 and 11 mono-specific specimens were analysed after ultrasonic cleaning in deionized water. All data are reported relative to the Vienna Pee Dee Belemnite standard (VPDB). External analytical precision, based on replicate analyses of in-house standards calibrated to NBS-19, is better than $\pm 0.1\%$ for $\delta^{18}\text{O}$ and $\delta^{13}\text{C}$.

Early Eocene through to middle Eocene sediments at ODP Site 1258 (Demerara rise) host well preserved benthic foraminifera⁸. *Cibicidoides subspiratus* was used as the primary species for stable isotope analysis. However, in certain intervals, notably in the younger part of our record (after 48.5 Myr ago), a decline in abundance of *C. subspiratus* dictated that we also use *C. eoceanus*. Although modern core top samples show significant inter-species stable isotope offsets between certain species of *Cibicidoides*³¹, our calculated inter-species offsets for the two Eocene species of *Cibicidoides* (from paired mono-specific analyses, $n = 168$) are statistically indistinguishable from zero for both $\delta^{18}\text{O}$ and $\delta^{13}\text{C}$ ($\delta^{18}\text{O} = -0.031$ ($1\sigma = 0.128$); $\delta^{13}\text{C} = 0.009$ ($1\sigma = 0.133$)). This provides justification for our strategy of using these two species in combination. Benthic foraminiferal taxonomy follows that of refs 32 and 33.

All $\delta^{18}\text{O}$ data are corrected to equilibrium calcite using the *Oridorsalis* spp. – *Cibicidoides* spp. correction factor of $+0.28\%$ derived from an assessment of isotopic offsets for Eocene benthic foraminifera³⁴. Use here of this correction factor is based on evidence (summarized in ref. 8) that Eocene *Oridorsalis umbonatus* secreted its calcite in $\delta^{18}\text{O}$ equilibrium with sea water. Palaeotemperatures were calculated using equation (1) of ref. 35. This equation provides excellent agreement with a global core top *Cibicidoides* spp. $\delta^{18}\text{O}$ calibration for a temperature range from 0 to 7 °C (ref. 35). In keeping with the view that there were no significant continental ice sheets during the early to early middle Eocene^{36,37}, our $\delta^{18}\text{O}$ records can be interpreted in terms of change in bottom water temperature at Demerara rise.

Age models. Drilling at Site 1258 recovered an unusually continuous, relatively expanded (sedimentation rates up to 2.5 cm kyr^{-1}) sedimentary section across the lower to middle Eocene boundary with unprecedented magneto-, bio- and cyclostratigraphic control for this interval^{138–40}. We developed an astronomically calibrated age model for Site 1258 by tuning clear and pronounced obliquity (~ 40 -kyr) cycles in the magnetostratigraphically calibrated magnetic susceptibility (MS) time series (Supplementary Fig. 1a) to computed obliquity cycles from the most recent astronomical solution⁴¹. Our tuning strategy is validated by the presence in our tuned MS time series of substantial power (and coherency with our tuning target) at frequencies of 23, 21 and 19 kyr (precession), 54 kyr (obliquity) and 96 kyr (eccentricity) (Supplementary Fig. 1b), even though these frequencies were not used in the tuning process. An absolute calibration to the astronomical solution is, at present, unattainable for the early to middle Eocene because of limitations in the precision of computed orbital variations pre-40 Myr ago⁴¹ and because of significant uncertainties in radiometric age calibrations^{42,43}. Consequently, we develop a 'floating' astronomically tuned timescale, using the C21r/C22n magnetochron boundary (age = 49.037 Myr ago⁴²) identified at Site 1258³⁹ as our anchor point.

Age models for the estimated CaCO_3 (%) records for ODP 1267 (Walvis ridge) and ODP 1210 (Shatsky rise) are derived by correlating the stratigraphic position of a biostratigraphic datum (LAD of the nannofossil *Discoaster lodoensis*) at both

of these sites to its position at Site 1258 (Supplementary Table 1). Further age model refinement was achieved by tuning clear, correlatable events in CaCO_3 (%) records from Sites 1267 and 1210 to the astronomically calibrated CaCO_3 (%) record from Site 1258 (Supplementary Tables 2 and 3). This tuning strategy was held as relaxed as possible, using a minimum of tie points.

Eocene records of CaCO_3 concentrations. We use sediment colour and magnetic susceptibility data in conjunction with measurements of sediment CaCO_3 content³⁸ to calculate, by regression, sediment CaCO_3 content at high resolution at Demerara rise (Fig. 1d; Supplementary Fig. 2e). We use comparable data^{44,45} to perform the same regressions for two other deep sea drill sites (ODP 1267, Walvis ridge, southern Atlantic and ODP 1210, Shatsky rise, central Pacific) (Supplementary Fig. 2f and g). At all three sites, estimated CaCO_3 concentrations prove to be a good predictor of measured CaCO_3 concentrations (Supplementary Fig. 2a–c). For methods for calculating CaCO_3 dissolution from our Eocene CaCO_3 records, see Supplementary Information.

- Curry, W. B., Slowey, N. C. & Lohmann, G. P. Oxygen and carbon isotopic fractionation of aragonitic and calcitic benthic foraminifera on Little Bahama Bank, Bahamas. *Eos* **74**, 368 (1993).
- Tjalsma, R. C. & Lohmann, G. P. *Paleocene-Eocene Bathyal and Abyssal Benthic Foraminifera from the Atlantic Ocean* (Micropaleontol. Spec. Publ. Ser., Vol. 4, Micropaleontol. Proj., New York, 1983).
- van Morkhoven, F. P. C. M., Berggren, W. A. & Edwards, A. S. Cenozoic cosmopolitan deep water benthic foraminifera. *Bull. Cent. Rech. Explor. Prod. Elf-Aquitaine* **11** (Pau, France, 1986).
- Katz, M. E. et al. Early Cenozoic benthic foraminiferal isotopes: species reliability and interspecies correction factors. *Paleoceanography* **18**, 1024, doi:10.1029/2002PA000798 (2003).
- Bemis, B. E., Spero, H. J., Bijma, J. & Lea, D. W. Reevaluation of the oxygen isotopic composition of planktonic foraminifera: experimental results and revised paleotemperature equations. *Paleoceanography* **13**, 150–160 (1998).
- Zachos, J., Pagani, M., Sloan, L., Thomas, E. & Billups, K. Trends, rhythms, and aberrations in global climate 65 Ma to present. *Science* **292**, 686–693 (2001).
- Browning, J. V., Miller, K. G. & Pak, D. K. Global implications of lower to middle Eocene sequence boundaries on the New Jersey coastal plain: the icehouse cometh. *Geology* **24**, 639–642 (1996).
- Shipboard Scientific Party, 2004. Site 1258. *Proc. ODP Init. Rep.* 207, 1–117 doi:10.2973/odp.proc.ir.207.105.2004 (2004).
- Suganuma, Y. & Ogg, J. G. Campanian through Eocene magnetostratigraphy of Sites 1257–1261, ODP Leg 207, Demerara Rise (western equatorial Atlantic). *Proc. ODP Sci. Res.* 207 (2006); available at (http://www-odp.tamu.edu/publications/207_SR/102/102.htm).
- Westerhold, T. & Röhl, U. High resolution cyclostratigraphy of the early Eocene — new insights into the origin of the Cenozoic cooling trend. *Clim. Past* **5**, 309–327 (2009).
- Laskar, J. et al. A long-term numerical solution for the insolation quantities of the Earth. *Astron. Astrophys.* **428**, 261–285 (2004).
- Berggren, W., Kent, D. & Swisher, C. III. in *Geochronology Time Scales and Global Stratigraphic Correlation* (ed. Berggren, W.) 129–212 (Society for Sedimentary Geology, Tulsa, 1995).
- Machlus, M., Hemming, S. R., Olsen, P. E. & Christie-Blick, N. Eocene calibration of geomagnetic polarity time scale reevaluated: evidence from the Green River Formation of Wyoming. *Geology* **32**, 137–140 (2004).
- Shipboard Scientific Party, 2004. Site 1267. *Proc. ODP Init. Rep.* 208, 1–77 doi:10.2973/odp.proc.ir.208.108.2004 (2004).
- Shipboard Scientific Party, 2002. Site 1210. *Proc. ODP Init. Rep.* 198, 1–89 doi:10.2973/odp.proc.ir.198.106.2002 (2002).